Supporting Information

Exploring Covalent Allosteric Inhibition of Antigen 85C from *Mycobacterium tuberculosis* by Ebselen Derivatives

*Christopher M. Goins[1], Steven Dajnowicz[1, 2], Sandeep Thanna[1], Steven J. Sucheck[1], Jerry M. Parks[3], and Donald R. Ronning[1]**

Table of Contents

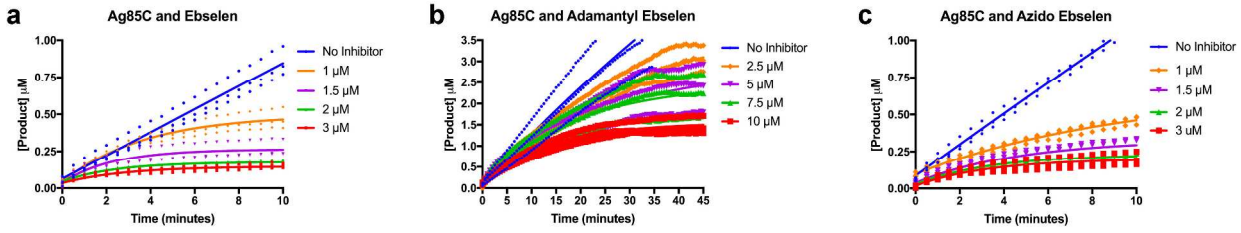

Supplemental figure 1: Progress curves for k_{inact}/K_I determination. (a-c) Data is plotted as a function of triplicate reads; fitted trend line is also given.

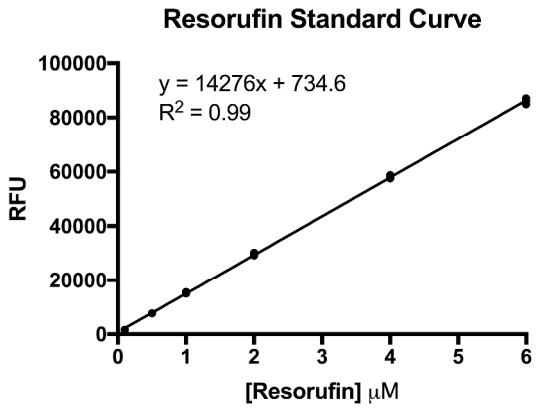

Supplemental figure 2: Resorufin standard curve: Resorufin was resuspended in DMSO and serial diluted. Flourescent reads were obtained using λ_{ex} = 500 nm with λ_{em} monitored at 590 nm and are displayed as triplicate points. Data were fit using linear regression.

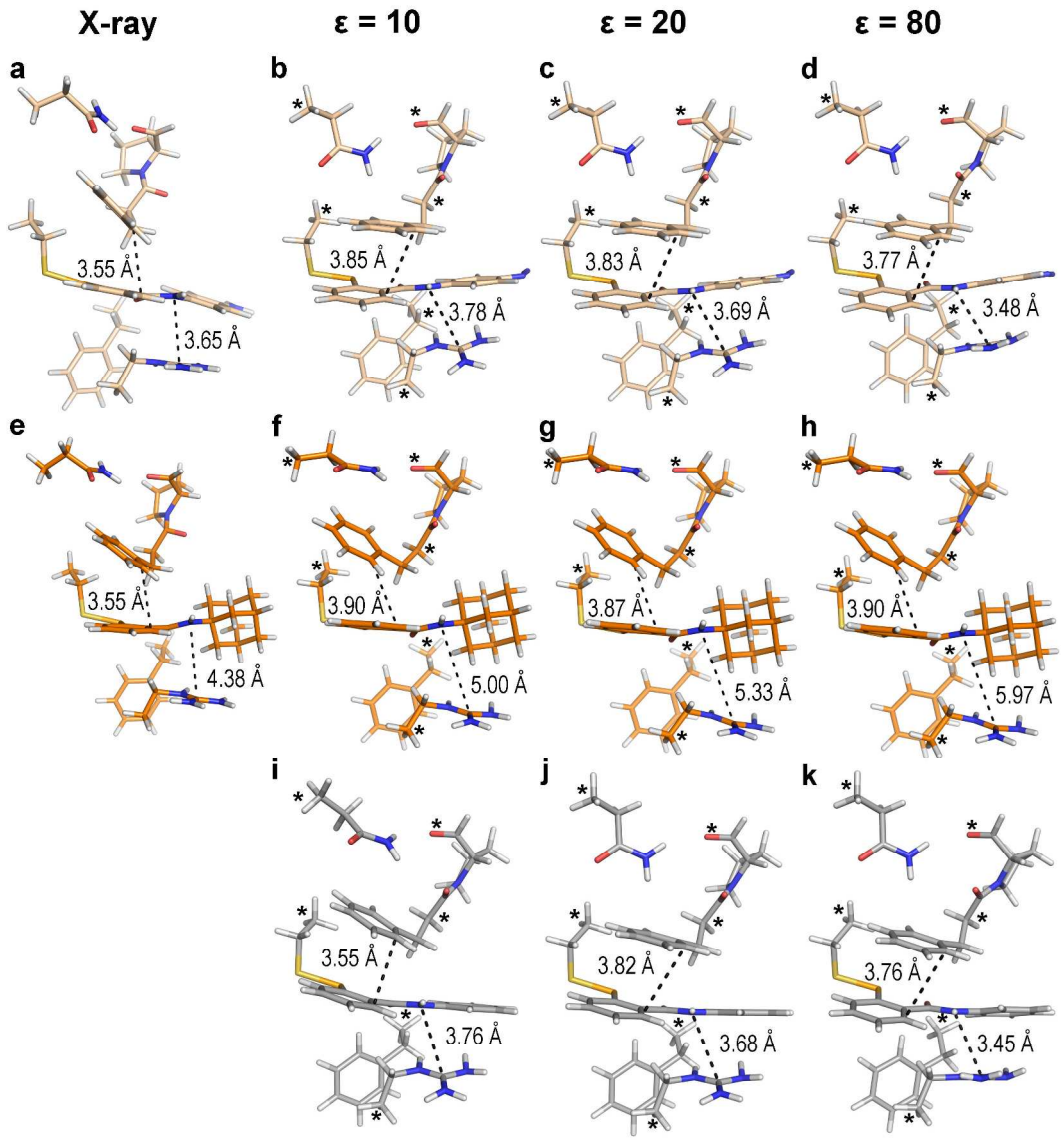

Supplemental Figure 3: QM geometry optimization for allosteric site residues and resulting distances. Coordinates for fixed atoms are indicated (*). Dielectric constant increases left to right, excluding the X-ray structure. (a-d) are Ag85C-Azido ebselen. (e-h) are Ag85C-Adamantyl ebselen. (i-j) are Ag85C-Ebselen.

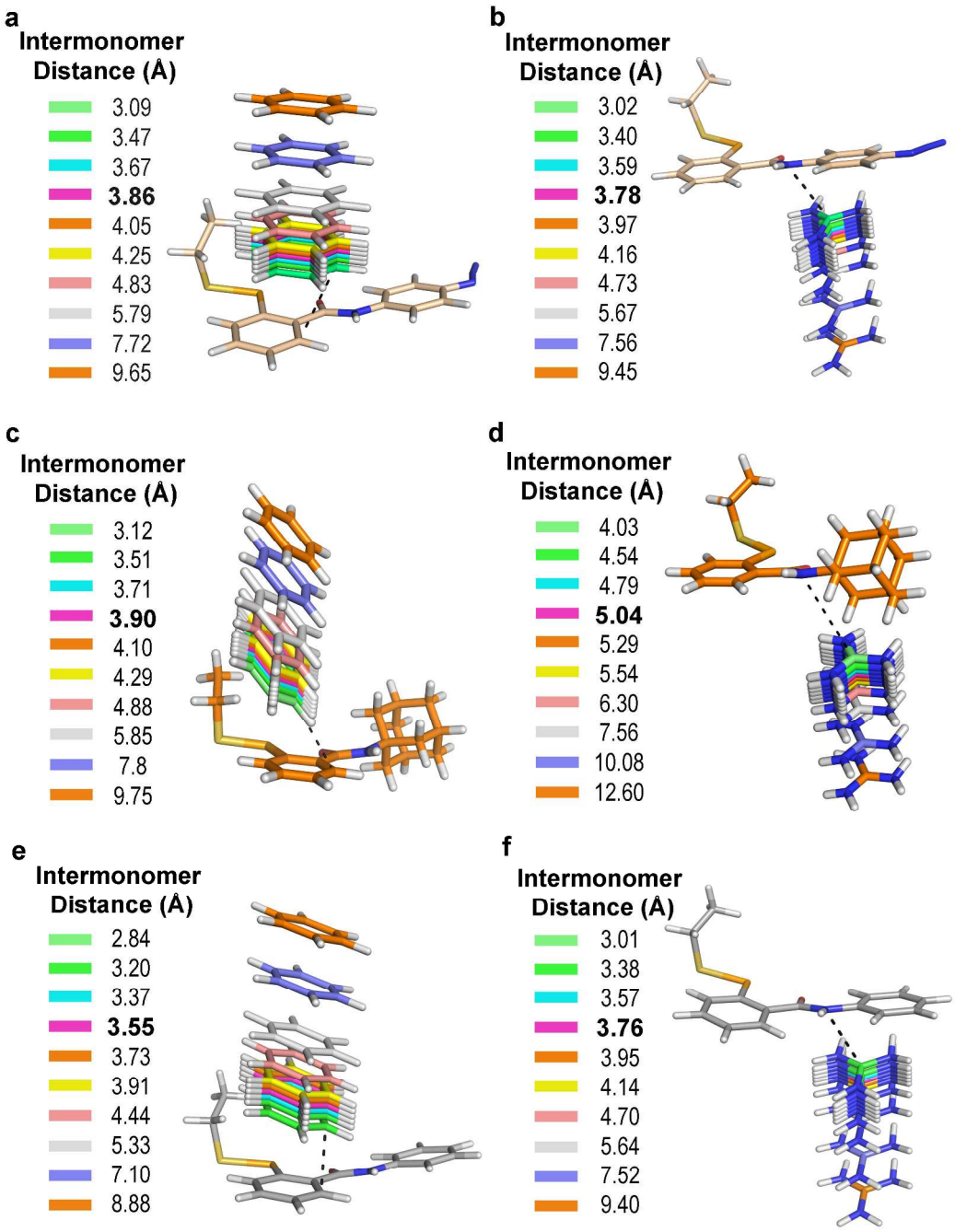

Supplemental Figure 4: Geometries of respective dimers for interaction energy calculations. Distances are color coded with respect to either benzene (Phe254) or guanidinium (Arg239). The bold distance corresponds to equilibrium distance in condensed phase. (a) Phe254 - azido ebselen

dimer. (b) Arg239 - azido ebselen dimer. (c) Phe254 - adamantyl ebselen dimer. (d) Arg239 - adamantyl dimer. (e) Phe254 – ebselen. (f) Arg239 – ebselen.

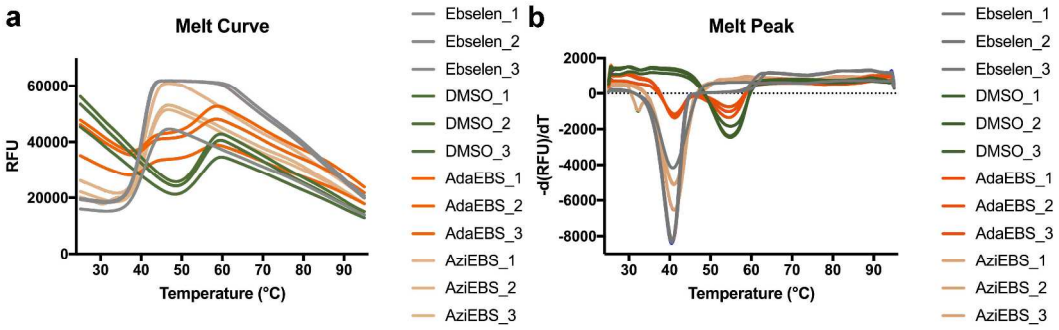

Supplemental Figure 5: (a) Raw triplicate data for the obtained melt curves. (b) Resulting melt peaks from DSF. DMSO corresponds to sample with No Drug Added.

Supplemental Methods: DFT Calculations

To compute the interaction energy between the two covalent modifiers (adamantyl ebselen and azido ebselen) and the two allosteric site residues (Phe254 and Arg239), we performed quantum chemical cluster calculations from the X-ray co-crystal structures (PDB entry 5KWJ (Ag85C-azido) and 5KWI (Ag85C-adamantyl). The quantum cluster of the allosteric sites contained the covalent modifier and five allosteric site residues (Asn211, Arg239, Phe254, Phe252, and Pro255). In each model, Cys209 (covalently modified), Asn211 and Phe252 were truncated at Cα and the free valences were capped with hydrogens (Figure S1). Similarly, Arg239 was truncated at Cγ (Figure S1). Additionally, the backbone atoms from the Cα of Phe254 through the carbonyl oxygen of Pro255 were retained in each model (Figure S1) and the carbonyl oxygen of Pro255 was modeled as an aldehyde. As a result, the Ag85C-adamantyl ebselen and Ag85C-azido ebselen quantum cluster models included 128 and 116 atoms, respectively. The geometry of each model was optimized at the BLYP-D3BJ/Def2-TZVP

level of theory[1-5]. During the optimization, the Cα atoms of residues Cys209, Asn211, Phe252, and Phe254 were constrained, as were the Cγ atoms of Arg239 and the carbonyl oxygen of Pro255. The geometry optimizations were performed with the SMD polarizable continuum solvent model with three different dielectric constants, ε = 10, 20, or 80[6]. From the ε = 10 optimized models, Phe254 – azido ebselen, Arg239 – azido ebselen, Phe254 - adamantyl ebselen, and Arg239 - adamantyl ebselen dimers were extracted to compute interaction energies. For the interaction energy calculations, Phe254 was modeled as benzene, Arg239 was modeled as guanidinium, and the covalent modifier was truncated at the Cα of Cys209.

It was shown previously that DFT with empirical dispersion corrections reproduces highly accurate non-covalent interaction energies for biologically relevant dimers to within ~0.2 kcal/mol[7]. Basis set superposition error is expected to be small for DFT calculations with a large basis set. Indeed, we found that the BSSE was < 0.1 kcal/mol (data not shown). Thus, these effects/corrections were neglected in all further calculations.

Noncovalent interaction energies (E_{int}) for SMD ε = 10 models were then computed according to the equation:

$$\Delta E_{int} = E_{complex} - E_{covalent\ modifier} - E_{Arg239\ or\ Phe254}$$

To generate interaction energy curves, an intermonomer distance was required for each interaction. Distances were measured between the closest carbon atom of the benzene ring (Phe254) and C3 of the primary benzylic ring of both ebselen derivatives. For the Arg interactions, the distance between the nitrogen of the amide linkage of both derivatives to the central carbon of the guanidinium was used. We defined a vector normal to the plane defined by three atoms of the allosteric site residue and scaled the interaction distance by moving the

fragment by a factor of 0.8, 0.9, 0.95, 1.0, 1.05, 1.1, 1.25, 1.5, 2.0 and 2.5 times the equilibrium distance (Figure S2). We then computed energies at each geometry without reoptimization at the SMD/BLYP-D3BJ/Def2-QZVP level of theory in both the gas-phase and with ε = 10. The resolution-of-the-identity (RI) approximation with the W06 auxiliary basis set was used to accelerate calculation of electron repulsion integrals in all calculations.

To assess the accuracy of our calculations for cation-π interaction energies, we computed the noncovalent interaction energy of NH_4^+ – benzene at the BLYP-D3BJ/Def2-QZVP level of theory in the gas-phase and compared it to a CCSD(T) reference interaction energy[8, 9]. The counterpoise-corrected CCSD(T) interaction energy of –17.5 kcal/mol was computed with the aug-cc-pVTZ basis set for carbon and nitrogen and the cc-pVTZ basis set for hydrogen[10, 11]. The BLYP-D3BJ/Def2-QZVP NH_4^+ – benzene interaction energy of -18.0 kcal/mol, reproduced the CCSD(T) value with an overestimation of 0.5 kcal/mol. An identical approach to assess the accuracy for π - π interaction energies was implemented for benzene-benzene interactions. The benchmark values for a parallel displaced benzene dimer is -2.62 kcal/mol and -2.71 kcal/mol for a T-shaped benzene dimer using CCSD(T)/CBS(Δa(DT)Z) level of theory[12]. The computed interaction energies using BLYP-D3BJ/Def2-QZVP are -3.18 and -2.60 kcal/mol, respectively. Thus, BLYP-D3BJ/Def2-QZVP has proven to efficiently compute noncovalent interaction energy for both cation - π and π - π interactions within reasonable error.

We also computed the reaction free energy, ΔG_r, for the oxidation reaction that occurs between Cys209 and the covalent modifier. Cys209 was modeled as ethylthiol in the free energy calculations. To obtain ΔG_r, the reactants (Cys209 and covalent modifier) and products were optimized at the SMD/M06-2X/TZVP level of theory with ε = 10. Following the geometry optimization, we performed vibration frequency calculations on the reactants and products to

confirm the presence of local minima and to compute thermochemical quantities. The M06-2X functional has been shown to perform accurately for thermochemical quantities for main group atoms[13]. All calculations were performed with Gaussian 09, Revision E.01 using an UltraFine grid and tight SCF convergence criteria [14,15].

Supplemental References

1. Becke, A. D. (1988) Density-functional exchange-energy approximation with correct asymptotic behavior, *Physical review A 38(6)*, 3098.
2. Lee, C., Yang, W., Parr, R. G. (1988) Development of the Colle-Salvetti correlation-energy formula into a functional of the electron density, *Phys. Rev. B 37(2)*, 785.
3. Grimme, S., Antony, J., Ehrlich, S., Krieg, H. (2010) A consistent and accurate ab initio parametrization of density functional dispersion correction (DFT-D) for the 94 elements H-Pu, *J. Chem. Phys. 132(15)*, 154104.
4. Grimme, S., Ehrlich, S., Goerigk, L. (2011) Effect of the damping function in dispersion corrected density functional theory, *J. Comput. Chem. 32(7)*, 1456-1465.
5. Weigend, F., Ahlrichs, R. (2005) Balanced basis sets of split valence, triple zeta valence and quadruple zeta valence quality for H to Rn: design and assessment of accuracy, *Phys. Chem. Chem. Phys. 7(18)*, 3297-3305.
6. Marenich, A. V., Cramer, C. J., and Truhlar, D. G. (2009) Universal solvation model based on solute electron density and on a continuum model of the solvent defined by the bulk dielectric constant and atomic surface tensions, *J. Phys. Chem B 113(18)*, 6378-6396.
7. Goerigk, L., Kruse, H., Grimme, S. (2011) Benchmarking Density Functional Methods against the S66 and S66x8 Datasets for Non□Covalent Interactions, *ChemPhysChem 12(17)*, 3421-3433.
8. Raghavachari, K., Trucks, G., Pople, J., Head-Gordon, M. (1989), A Fifth-order Perturbation Comparison of Electron Correlation Theories, *Chem. Phys. Lett. 157(1)*, 479–483.
9. Ansorg, K., Tafipolsky, M, Engels, B. (2013) Cation-pi Interactions: Accurate intermolecular potential from symmetry-adapted perturbation theory. *J. Phys Chem B 117(35)*, 10093-10102
10 Dunning, T. J. Jr. (1989) Gaussian Basis Sets for Use in Correlated Molecular Calculations. I. The Atoms Boron Through Neon and Hydrogen, *J. Chem. Phys. 90(1)*, 1007.
11. Kendall, R., Dunning, T., Jr., Harrison, R.J. (1992) Electron affinities of the first-row atoms revisited. Systematic basis sets and wave functions, *J. Chem. Phys.* 96(1), 6796-6806.
12. Takatani, T., Hohenstein, E. G., Malagoli, M., Marshall, M. S., Sherrill, C. D. (2010) Basis set consistent revision of the S22 test set of noncovalent interaction energies, *J. Chem. Phys 132*. 144104
13. Zhao, Y., Truhlar, D. G. (2008) The M06 suite of density functionals for main group heterochemistry, thermochemical kinetics, noncovalent interactions, excited states, and transition elements: two new functionals and systematic testing of four M06-class functionals and 12 other functionals. *Theor Chem Account 120*, 215-241
14. Weigend, F. (2006) Accurate Coulomb-fitting basis sets for H to Rn, *Phys. Chem. Chem. Phys. 8(9)*, 1057-1065.

15. Frisch, M. J., Trucks, G. W., Schlegel, H. B., Scuseria, G. E., Robb, M. A., Cheeseman, J. R., Scalmani, G., Barone, V., Mennucci, B., Petersson, G. A., Nakatsuji, H., Caricato, M., Li, X., Hratchian, H. P., Izmaylov, A. F., Bloino, J., Zheng, G., Sonnenberg, J. L., Hada, M., Ehara, M., Toyota, K., Fukuda, R., Hasegawa, J., Ishida, M., Nakajima, T., Honda, Y., Kitao, O., Nakai, H., Vreven, T., Montgomery, J. A., Jr., Peralta, J. E., Ogliaro, F., Bearpark, M., Heyd, J. J., Brothers, E., Kudin, K. N., Staroverov, V. N., Kobayashi, R., Normand, J., Raghavachari, K., Rendell, A., Burant, J. C., Iyengar, S. S., Tomasi, J., Cossi, M., Rega, N., Millam, J. M., Klene, M., Knox, J. E., Cross, J. B., Bakken, V., Adamo, C., Jaramillo, J., Gomperts, R., Stratmann, R. E., Yazyev, O., Austin, A. J., Cammi, R., Pomelli, C., Ochterski, J. W., Martin, R. L., Morokuma, K., Zakrzewski, V. G., Voth, G. A., Salvador, P., Dannenberg, J. J., Dapprich, S., Daniels, A. D., Farkas, Ö., Foresman, J. B., Ortiz, J. V., Cioslowski, J., Fox, D. J. (2009) Gaussian 09, Revision E.01, *Gaussian, Inc. Wallingford CT*.